

Model of Collagen Flow through Convergent and Divergent Planar Channel

Bc. Jan Frouz

supervisor: Ing. Jan Skočilas, Ph.D.

Abstract: *The aim of this work is to implement finite difference method with Upper Convected Maxwell constitution equation in MATLAB and provide mathematical model of flow of collagen matter trough convergent and divergent planar channel. It was necessary to transform solved geometry from non-orthogonal grid to orthogonal grid. Due to creep flow conditions, velocity field had been carried out via power model. Central and upwind finite difference scheme of first and second order had been used. This collagen flow model is prepared to be used in the future for optimization of physical attributes of collagen matter in cooperation with the laboratory experiment.*

Keywords: *finite difference method, rheology, collagen, convergent divergent planar channel, Upper Convected Maxwell*

1 Introduction

Although collagen is the most abundant mammalian protein accounting for 20-30% of total body protein [1], has been widely used in many applications and has been carefully studied, it's rheological properties still remain unknown.

Collagen is widely used in medical applications as carrier for delivery of drug, protein and gene. Collagen sponges are very useful as skin replacement, bone substitutes and bioengineered tissues, such as blood vessels, heart valves and ligaments. [2].

Gelse et al. wrote "the name 'collagen' is used as a generic term for proteins forming a characteristic triple helix of three polypeptide chains". Twenty-six genetically distinct types of collagen has been discovered. The most abundant group of collagens are represented by fibril-forming collagens (from type I to XI). Collagen I is the most plentiful and best studied collagen, it forms more than 90% of the organic mass of bone and is major collagen contained in skin, ligaments, cornea etc. [3].

In spite of knowing collagen so very well, knowledge about physical properties of collagen matter is very shallow. It may have thixotropic properties [4] and is visco-elastic [5]. Purpose of this work is to implement finite difference method with formulas proposed by Zitny [5] in MATLAB and provide simulation of flow of collagen matter trough convergent and divergent planar channel.

In the future this collagen flow model could be used for optimization of physical attributes of collagen matter in cooperation with laboratory experiment.

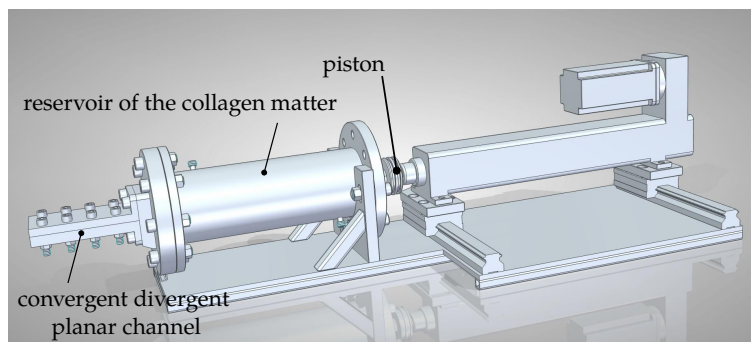


Figure 1 *Experimental device - capillary viscosimetr (courtesy of Bc. S. Solnář) [6].*

Mathematical model should predict pressure behavior which can be compared with results obtained on capillary viscosimeter with convergent and divergent planar channel. Experimental device is currently under development at Department of Process Engineering. Next step in the future will be to apply multi-objective optimization (for example PSO) with the mathematical model as fitness function to find range for physical properties of collagen matter.

2 Materials and methods

2.1 Governing equations

The collagen matter has visco-elastic behavior. This work is hugely influenced by work of Zitny [5] and Pavlovec [7] who introduced geometry transformation formulas from non-orthogonal geometry to orthogonal one, usage of Upper Convective Maxwell constitutive equations and have created physical model this work is based on. Equation following in this section are final formulas presented by Zitny [5]. On the figure 1 you can see basic geometry of convergent divergent planar channel (capillary rheometr) with simple grid. Fluid is flowing from left to right (parallel to x axis).

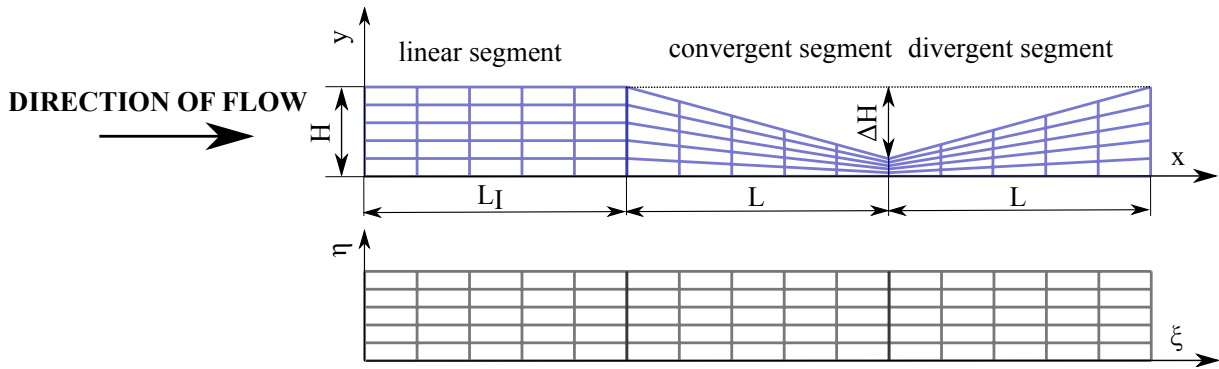


Figure 2 Grid transformation [5].

Table 1 Transformation constants

	straight	convergent	divergent
x_0	0	L_I	$L + L_I$
β	0	$-\frac{\Delta H}{H_0}$	$\frac{\Delta H}{H_0}$
ΔL	L_I	L	L
H_0	H	H	$H - \Delta H$

System transformation from non-orthogonal to orthogonal:

$$\xi = \frac{x - x_0}{\Delta L} \quad (1) \quad \eta = \frac{y}{H_0 \left(1 + \beta \frac{x - x_0}{\Delta L} \right)} \quad (2) \quad \varepsilon = \frac{H_0}{\Delta L} \quad (3)$$

Continuity equation:

$$\nabla \cdot u = 0 \quad (4)$$

Cauchy's equation:

$$\frac{\partial p}{\partial x} = \frac{\partial \tau_{xx}}{\partial x} + \frac{\partial \tau_{xy}}{\partial y} \quad (5) \quad \frac{\partial p}{\partial y} = \frac{\partial \tau_{yy}}{\partial y} + \frac{\partial \tau_{yx}}{\partial x} \quad (6)$$

Viscosity approximation:

$$\mu(II) = K \left(\sqrt{2 \left(\frac{\partial u_x}{\partial x} \right)^2 + 2 \left(\frac{\partial u_y}{\partial y} \right)^2 + \left(\frac{\partial u_y}{\partial x} + \frac{\partial u_x}{\partial y} \right)^2} \right)^{n-1} \quad (7)$$

Due to creep flow power approximation model of velocity had been chosen. Because the zero point of coordinate system had been placed in the bottom plane of rheometer (see figure 1) different equations had to written for velocity in the bottom half of the rheometer and in the top part of the rheometer.

$$u_m = \frac{\dot{V}(2n+1)}{H_0(n+1)} \quad (8)$$

$$u_x = \frac{u_m}{1+\beta\xi} (1 - (1-2\eta)^{\frac{n+1}{n}}), \quad \eta < 0.5 \quad (9)$$

$$u_x = \frac{u_m}{1+\beta\xi} (1 - (2\eta-1)^{\frac{n+1}{n}}), \quad \eta > 0.5 \quad (10)$$

$$u_y = \frac{\varepsilon\beta u_m}{1+\beta\xi} \eta (1 - (1-2\eta)^{\frac{n+1}{n}}), \quad \eta < 0.5 \quad (11)$$

$$u_y = \frac{\varepsilon\beta u_m}{1+\beta\xi} \eta (1 - (2\eta-1)^{\frac{n+1}{n}}), \quad \eta > 0.5 \quad (12)$$

Constitutive equations:

$$2\mu(II) \frac{\partial u_x}{\partial x} = \tau_{xx} + \frac{\mu(II)}{G} \left(\frac{u_x}{\Delta L} \left(\frac{\partial \tau_{xx}}{\partial \xi} - \frac{\eta\beta}{(1+\beta\xi)} \frac{\partial \tau_{xx}}{\partial \eta} \right) + \frac{u_y}{\Delta L \varepsilon (1+\beta\xi)} \frac{\partial \tau_{xx}}{\partial \eta} - 2 \frac{\partial u_x}{\partial x} \tau_{xx} - 2 \frac{\partial u_x}{\partial y} \tau_{xy} \right) \quad (13)$$

$$2\mu(II) \frac{\partial u_y}{\partial y} = \tau_{yy} + \frac{\mu(II)}{G} \left(\frac{u_x}{\Delta L} \left(\frac{\partial \tau_{yy}}{\partial \xi} - \frac{\eta\beta}{(1+\beta\xi)} \frac{\partial \tau_{yy}}{\partial \eta} \right) + \frac{u_y}{\Delta L \varepsilon (1+\beta\xi)} \frac{\partial \tau_{yy}}{\partial \eta} - 2 \frac{\partial u_y}{\partial x} \tau_{xy} - 2 \frac{\partial u_y}{\partial y} \tau_{yy} \right) \quad (14)$$

$$\mu(II) \left(\frac{\partial u_x}{\partial y} + \frac{\partial u_y}{\partial x} \right) = \tau_{xy} + \frac{\mu(II)}{G} \left(\frac{u_x}{\Delta L} \left(\frac{\partial \tau_{xy}}{\partial \xi} - \frac{\eta\beta}{(1+\beta\xi)} \frac{\partial \tau_{xy}}{\partial \eta} \right) + \frac{u_y}{\Delta L \varepsilon (1+\beta\xi)} \frac{\partial \tau_{xy}}{\partial \eta} - \frac{\partial u_y}{\partial x} \tau_{xx} - \frac{\partial u_x}{\partial y} \tau_{yy} \right) \quad (15)$$

2.2 Border conditions

Bottom of the rheometer:

$$\tau_{xx} = \frac{2\mu(II)^2}{G} \left(\frac{\partial u_x}{\partial y} \right)^2 \quad (16)$$

$$\tau_{yy} = 0 \quad (17)$$

$$\tau_{xy} = \mu(II) \frac{\partial u_x}{\partial y} \quad (18)$$

Top of the rheometer:

$$\begin{pmatrix} 1 - \frac{2\mu(II)}{G} \left(\frac{\partial u_x}{\partial x} \right) & 0 & -\frac{2\mu(II)^2}{G} \left(\frac{\partial u_x}{\partial y} \right) \\ 0 & 1 - \frac{2\mu(II)}{G} \left(\frac{\partial u_y}{\partial y} \right) & -\frac{2\mu(II)}{G} \left(\frac{\partial u_y}{\partial x} \right) \\ -\frac{2\mu(II)}{G} \left(\frac{\partial u_y}{\partial x} \right) & -\frac{2\mu(II)}{G} \left(\frac{\partial u_x}{\partial y} \right) & 1 \end{pmatrix} \begin{pmatrix} \tau_{xx} \\ \tau_{yy} \\ \tau_{xy} \end{pmatrix} = \begin{pmatrix} 2\mu(II) \frac{\partial u_x}{\partial x} \\ 2\mu(II) \frac{\partial u_y}{\partial y} \\ 2\mu(II) \left(\frac{\partial u_x}{\partial x} + \frac{\partial u_y}{\partial y} \right) \end{pmatrix} \quad (19)$$

Entrance conditions:

$$\tau_{xx} = \frac{2\mu(II)^2}{G} \left(\frac{\partial u_x}{\partial y} \right)^2 \quad (20) \quad \tau_{yy} = 0 \quad (21) \quad \tau_{xy} = \mu(II) \frac{\partial u_x}{\partial y} \quad (22)$$

3 Finite difference method

For solving formulas (13) (14) and (15) finite difference method (FDM) had been chosen. FDM is relatively easy to implement. First order approximation formulas were used in "approximation approach" (see later) to solve column $j = 2$, $j = n_y - 1$ and row $i = 2$, everything else (except border) was carried out by second order approximation.

$$\frac{\partial \tau_{kk}^{i,j}}{\partial \eta} = \frac{\tau_{kk}^{i,j+1} - \tau_{kk}^{i,j-1}}{2\Delta\eta}, \quad (23) \quad \frac{\partial \tau_{kk}^{i,j}}{\partial \eta} = \frac{\frac{1}{12}\tau_{kk}^{i,j-2} - \frac{2}{3}\tau_{kk}^{i,j-1} + \frac{2}{3}\tau_{kk}^{i,j+1} - \frac{1}{12}\tau_{kk}^{i,j+2}}{\Delta\eta} \quad (25)$$

$$\frac{\partial \tau_{kk}^{i,j}}{\partial \xi} = \frac{\tau_{kk}^{i,j} - \tau_{kk}^{i-1,j}}{\Delta\xi}, \quad (24) \quad \frac{\partial \tau_{kk}^{i,j}}{\partial \xi} = \frac{\frac{1}{2}\tau_{kk}^{i-2,j} - 2\tau_{kk}^{i-1,j} + \frac{3}{2}\tau_{kk}^{i,j}}{\Delta\xi} \quad (26)$$

$$\frac{u_y}{\Delta L \varepsilon (1 + \beta \xi)} \frac{\partial \tau_{kk}^{i,j}}{\partial \eta} = \frac{2|u_y| \tau_{kk}^{i,j} + (u_y - |u_y|) \tau_{kk}^{i,j+1} - (u_y + |u_y|) \tau_{xx}^{i,j-1}}{2\Delta L \varepsilon (1 + \beta \xi)} \quad (27)$$

In the first approach we tried to approximate formula (27) just by central difference, but results behaved very strangely. Afterwards backward or forward scheme was used, depending on u_y orientation, which gave much more reasonable numbers. Direction of u_y can not be neglected.

Formulas (23) could be used in explicit or implicit way. Both approaches had been tried.

3.1 Implicit scheme

Implicit scheme has larger round-off errors compared to explicit scheme, is more difficult to implement and costs more resources. However predictor is not necessary and implicit scheme is always stable. If we use approximation formulas (23-27) on constitutive equations (13-15) it can be expressed as follows:

$$\begin{aligned} A &= \frac{\mu u_x}{G \Delta L \Delta \xi}, & B &= \frac{|u_y| \mu}{\Delta \eta \Delta L \varepsilon (1 + \beta \xi) G}, & D &= \frac{(u_y - |u_y|)}{G \varepsilon \Delta L (1 + \beta \xi) 2 \Delta \eta} \\ U &= -\frac{2\mu}{G}, & C &= \frac{\mu u_x \eta \beta}{G \Delta L (1 + \beta \xi) 2 \Delta \eta}, & E &= \frac{(u_y + |u_y|)}{G \varepsilon \Delta L (1 + \beta \xi) 2 \Delta \eta} \end{aligned}$$

$$\tau_{xx}^{i,j}(1 + A + B + U \frac{\partial u_x}{\partial x}) + (D - C)\tau_{xx}^{i,j+1} - (E + C)\tau_{xx}^{i,j-1} + U\tau_{xy}^{i,j} = 2\mu(II) \frac{\partial u_x}{\partial x} + A\tau_{xx}^{i-1,j} \quad (28)$$

$$\tau_{yy}^{i,j}(1 + A + B + U \frac{\partial u_x}{\partial x}) + (D - C)\tau_{yy}^{i,j+1} - (E + C)\tau_{yy}^{i,j-1} + U\tau_{xy}^{i,j} = 2\mu(II) \frac{\partial u_x}{\partial x} + A\tau_{yy}^{i-1,j} \quad (29)$$

$$\tau_{xy}^{i,j}(1 + A + B) + (D - C)\tau_{xy}^{i,j+1} - (E + C)\tau_{xy}^{i,j-1} + U \frac{\partial u_y}{\partial x} \tau_{xx}^{i,j} + U \frac{\partial u_x}{\partial y} \tau_{yy}^{i,j} = \mu(II) \left(\frac{\partial u_y}{\partial x} + \frac{\partial u_x}{\partial y} \right) + A\tau_{xy}^{i-1,j} \quad (30)$$

This can be written into following matrix:

$$\begin{pmatrix} 1 + A + B + U \frac{\partial u_x}{\partial x} & 0 & \frac{\partial u_x}{\partial y} & (D - C) & 0 & 0 & 0 & 0 & 0 \\ 0 & 1 + A + B + U \frac{\partial u_y}{\partial y} & \frac{\partial u_y}{\partial x} & 0 & (D - C) & 0 & 0 & 0 & 0 \\ \frac{\partial u_y}{\partial x} & \frac{\partial u_x}{\partial y} & (1 + A + B) & 0 & 0 & (D - C) & 0 & 0 & 0 \\ -(E + C) & 0 & 0 & 1 + A + B + U \frac{\partial u_x}{\partial x} & 0 & \frac{\partial u_x}{\partial y} & (D - C) & 0 & 0 \\ 0 & -(E + C) & 0 & 0 & 1 + A + B + U \frac{\partial u_y}{\partial y} & \frac{\partial u_y}{\partial x} & 0 & (D - C) & 0 \\ 0 & 0 & -(E + C) & \frac{\partial u_y}{\partial x} & \frac{\partial u_x}{\partial y} & (1 + A + B) & 0 & 0 & (D - C) \quad \dots \\ & & & & \vdots & & & & \end{pmatrix} \begin{pmatrix} \tau_{xx}^{j=2} \\ \tau_{yy}^{j=2} \\ \tau_{xy}^{j=2} \\ \tau_{xx}^{j+1} \\ \tau_{yy}^{j+1} \\ \tau_{xy}^{j+1} \\ \vdots \end{pmatrix} = \begin{pmatrix} A \cdot \tau_{xx}^{i-1,j} + 2\mu(II) \frac{\partial u_x}{\partial x} + (E + C)\tau_{xx}^{i,j-1} \\ A \cdot \tau_{yy}^{i-1,j} + 2\mu(II) \frac{\partial u_y}{\partial y} + (E + C)\tau_{yy}^{i,j-1} \\ A \cdot \tau_{xy}^{i-1,j} + \mu(II) \left(\frac{\partial u_x}{\partial y} + \frac{\partial u_y}{\partial x} \right) + (E + C)\tau_{xy}^{i,j-1} \\ A \cdot \tau_{xx}^{i-1,j} + 2\mu(II) \frac{\partial u_x}{\partial x} \\ A \cdot \tau_{yy}^{i-1,j} + 2\mu(II) \frac{\partial u_y}{\partial y} \\ A \cdot \tau_{xy}^{i-1,j} + \mu(II) \left(\frac{\partial u_x}{\partial y} + \frac{\partial u_y}{\partial x} \right) \\ \vdots \end{pmatrix} \quad (31)$$

3.2 Explicit approximation of constitutive equations

Explicit method for equations ((13)-(15)) has been carried out. It uses following predictor introduced by Zitny [5]:

$$\tau_{xx}^{i,j} \left(1 + \frac{\mu(II)}{G} \left(\frac{u_x}{\Delta L \Delta \xi} - 2 \frac{\partial u_x}{\partial x} \right) \right) = \frac{\mu(II)}{G} \left(\frac{u_x}{\Delta L \Delta \xi} \tau_{xx}^{i-1,j} + 2 \frac{\partial u_x}{\partial y} \tau_{xy}^{i,j} \right) + 2\mu(II) \frac{\partial u_x}{\partial x} \quad (32)$$

$$\tau_{yy}^{i,j} \left(1 + \frac{\mu(II)}{G} \left(\frac{u_x}{\Delta L \Delta \xi} - 2 \frac{\partial u_y}{\partial y} \right) \right) = \frac{\mu(II)}{G} \frac{u_x}{\Delta L \Delta \xi} \tau_{yy}^{i-1,j} + 2\mu(II) \frac{\partial u_x}{\partial x} \quad (33)$$

$$\tau_{xy}^{i,j} \left(1 + \frac{\mu(II)}{G} \frac{u_x}{\Delta L \Delta \xi} \right) = \frac{\mu(II)}{G} \frac{u_x}{\Delta L \Delta \xi} \tau_{xy}^{i-1,j} + 2\mu(II) \left(\frac{\partial u_x}{\partial x} + \frac{\partial u_y}{\partial y} \right) \quad (34)$$

Final discretization could be written in this manner:

$$\tau_{xx}^{i,j} = \frac{2\mu(II) \frac{\partial u_x}{\partial x} + \frac{\mu(II)}{G} \left(\frac{u_x}{\Delta L} \left(\frac{2\tau_{xx}^{i-1,j} - \frac{1}{2}\tau_{xx}^{i-2,j}}{\Delta \xi} + \frac{\frac{1}{2}\tau_{xx}^{i-2,j} - 2\tau_{xx}^{i-1,j} + \frac{3}{2}\tau_{xx}^{i,j}}{\Delta \eta} \right) - \left(\frac{(u_y - |u_y|)\tau_{xx}^{i,j+1} - (u_y + |u_y|)\tau_{xx}^{i,j-1}}{2\Delta \eta \Delta L \varepsilon (1 + \beta \xi)} \right) + \frac{\partial u_x}{\partial y} \tau_{xy} \right)}{1 + \frac{\mu(II)}{G} \left(\frac{3u_x}{2\Delta L \Delta \xi} + \frac{|u_y|}{\Delta \eta \Delta L \varepsilon (1 + \beta \xi)} - 2 \frac{\partial u_x}{\partial x} \tau_{xx} \right)} \quad (35)$$

$$\tau_{yy}^{i,j} = \frac{2\mu(II) \frac{\partial u_y}{\partial y} + \frac{\mu(II)}{G} \left(\frac{u_x}{\Delta L} \left(\frac{2\tau_{yy}^{i-1,j} - \frac{1}{2}\tau_{yy}^{i-2,j}}{\Delta \xi} + \frac{\frac{1}{2}\tau_{yy}^{i-2,j} - 2\tau_{yy}^{i-1,j} + \frac{3}{2}\tau_{yy}^{i,j}}{\Delta \eta} \right) - \left(\frac{(u_y - |u_y|)\tau_{yy}^{i,j+1} - (u_y + |u_y|)\tau_{yy}^{i,j-1}}{2\Delta \eta \Delta L \varepsilon (1 + \beta \xi)} \right) + \frac{\partial u_y}{\partial x} \tau_{xy} \right)}{1 + \frac{\mu(II)}{G} \left(\frac{3u_x}{2\Delta L \Delta \xi} + \frac{|u_y|}{\Delta \eta \Delta L \varepsilon (1 + \beta \xi)} - 2 \frac{\partial u_y}{\partial y} \tau_{yy} \right)} \quad (36)$$

$$\tau_{xy}^{i,j} = \frac{\mu(II) \left(\frac{\partial u_x}{\partial y} + \frac{\partial u_y}{\partial x} \right) + \frac{\mu(II)}{G} \left(\frac{u_x}{\Delta L} \left(\frac{2\tau_{xy}^{i-1,j} - \frac{1}{2}\tau_{xy}^{i-2,j}}{\Delta \xi} + \frac{\frac{1}{2}\tau_{xy}^{i-2,j} - 2\tau_{xy}^{i-1,j} + \frac{3}{2}\tau_{xy}^{i,j}}{\Delta \eta} \right) - \left(\frac{(u_y - |u_y|)\tau_{xy}^{i,j+1} - (u_y + |u_y|)\tau_{xy}^{i,j-1}}{2\Delta \eta \Delta L \varepsilon (1 + \beta \xi)} \right) + \frac{\partial u_x}{\partial y} \tau_{yy} + \frac{\partial u_y}{\partial x} \tau_{xx} \right)}{1 + \frac{\mu(II)}{G} \left(\frac{3u_x}{2\Delta L \Delta \xi} + \frac{|u_y|}{\Delta \eta \Delta L \varepsilon (1 + \beta \xi)} \right)} \quad (37)$$

There are two implemented variants of explicit model. The simplest way how to explain it is in figure 3. The first variant ("approximation" approach) where the second column and last-but-one column points (red) are obtained from first order approximation and second variant ("predictor approach"), where same points (red) are taken directly from predictor. Under these conditions, one might expect the first approach to find the solution faster, but the opposite behavior has been observed.

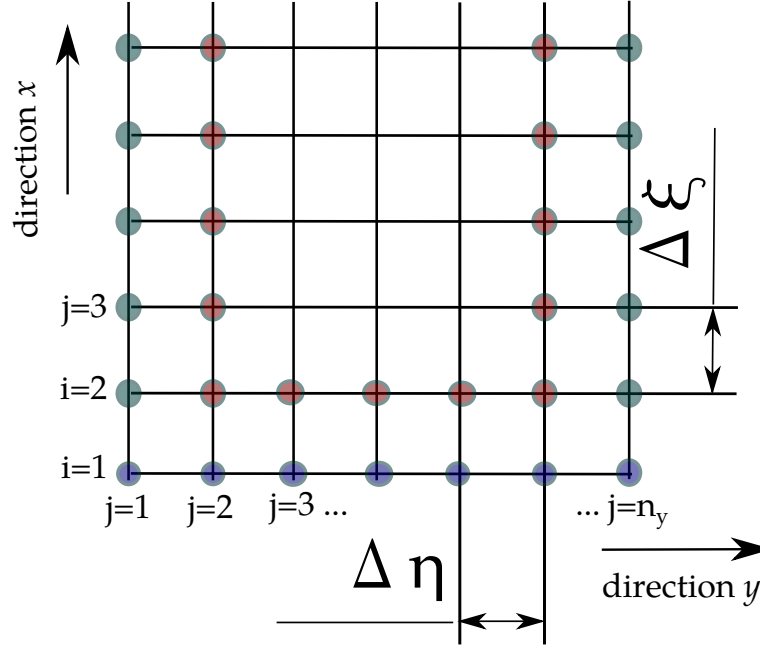


Figure 3 Mesh used for calculation. Red points have been approximated by neighbours or taken directly from predictor.

Then pressure can be calculated from stresses:

$$\begin{aligned}
 p = & \left(\frac{\tau_{xx}^{i,j} - \tau_{xx}^{i-1,j}}{\xi} - \frac{\eta\beta}{(1 + \beta\xi)} \frac{\tau_{xx}^{i,j+1} - \tau_{xx}^{i,j+1} \tau_{xx}^{i,j+1} \tau_{xx}^{i,j+1}}{2\Delta\eta} \right. \\
 & \left. + \varepsilon\eta\beta \frac{\tau_{xy}^{i,j} - \tau_{xy}^{i-1,j}}{\Delta\xi} + \frac{1 - (\varepsilon\eta\beta)^2}{\varepsilon(1 + \beta\xi)} + \frac{\tau_{xy}^{i,j+1} - \tau_{xy}^{i,j-1}}{3\Delta\eta} \right) \Delta\xi + p^{i-1,j} \quad (38)
 \end{aligned}$$

3.3 MATLAB implementation

FDM code has been implemented in MATLAB in two main codes, *main.m* and *segment.m*. Code *main.m* is responsible for input parameters, geometry of segments, starting segment code, transporting border conditions from one segment to another and viewing/printing the results. Code *segment.m* is implementing formulas for calculation of velocities, their derivations, viscosity, predictor, stresses, residue and pressure.

To speed up the code, parts of code were written in vectorized form. Bottlenecks were found using *profler* function [8]. The most time consuming (more than 60% of *segment.m*) is residue calculation.

3.4 Postprocessing - transformation of results back to non-orthogonal system

There is a concern to transform calculated data (pressure, velocities etc.) back to non-orthogonal system. There have been several approaches how to do it. Firstly, we tried to fit each row of result matrix (where sensible) with polynomial and then scale it to new length. Fitting with polynomial had been done by MATLAB function *polyfit*. For example the results of fitting $p(10, :)$ (pressure matrix in divergent segment on row 10) without scaling are in figure 4.

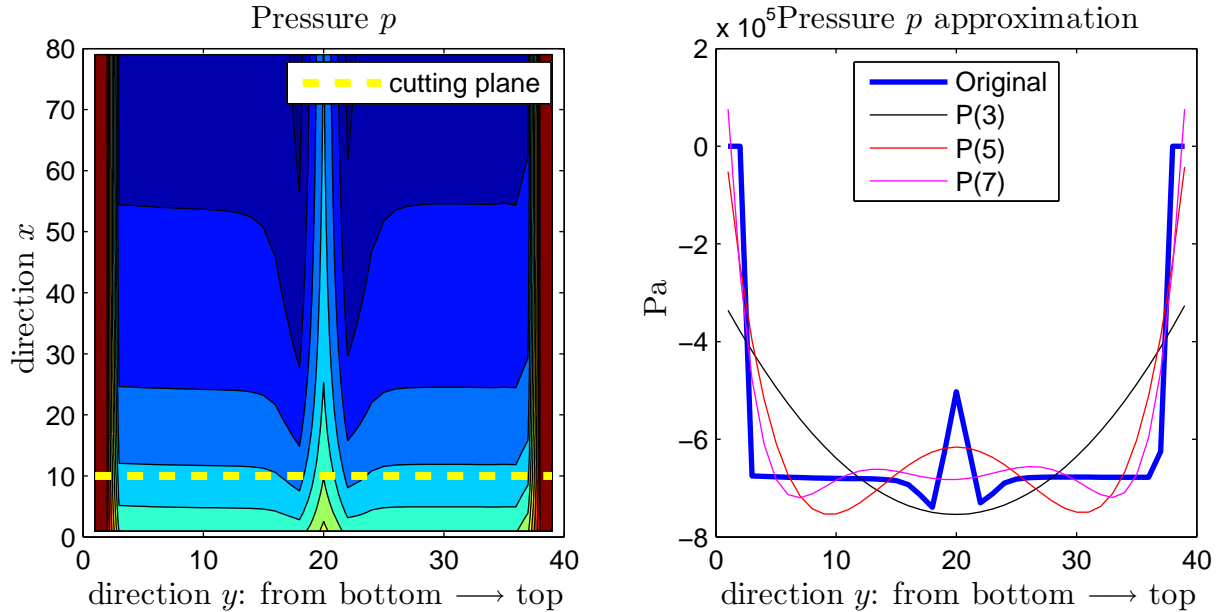


Figure 4 First approach. Approximation of pressure by polynomial.

However this approach was not very successful, it would be necessary to find better fitting function.

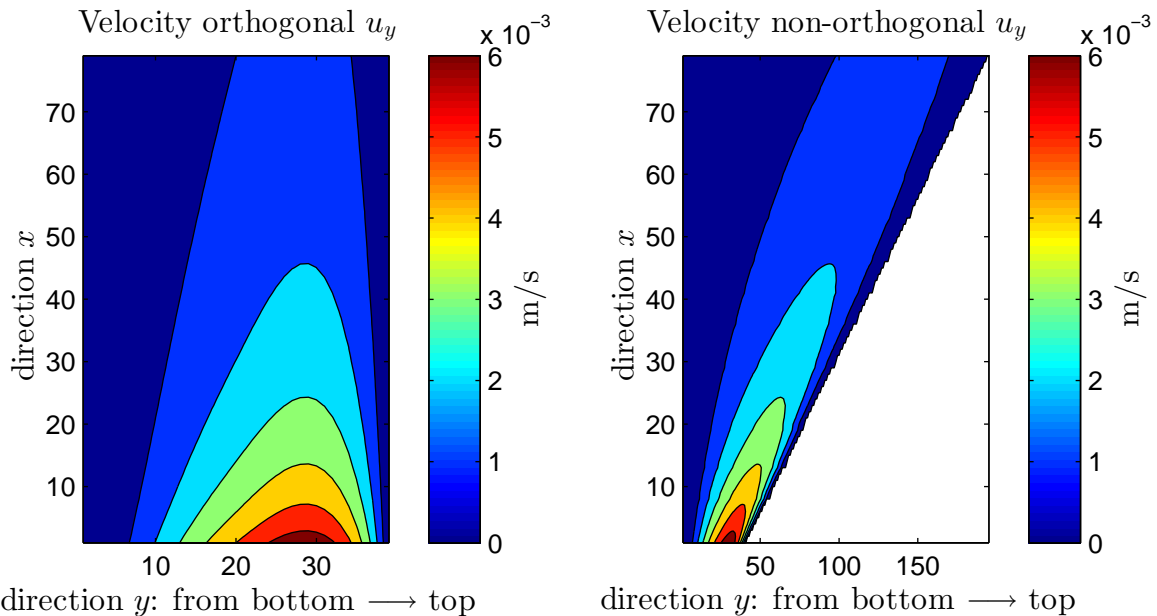


Figure 5 Transformation from orthogonal to nonorthogonal grid in divergent segment using 'ImWarp'.

In so far final approach MATLAB image transformation instruments has been used, specifically *ImWarp* to stretch each row of the original by aspect ratio. Produced matrix is naturally larger to preserve any important details from the original.

4 Results

Although implicit scheme was introduced in FDM chapter, implicit approximation seems to produce matrices which are badly scaled and singular to working precision. Another disadvantage compared with explicit method are higher round-off errors.

4.1 Explicit scheme results

Residue

First difference to observe between "approximation" and "predictor" approach are residue (see figure 6). Residue are defined by following equations:

$$R_{\tau_{ij}}^0 = \tau_{ij}^{k=0} \quad (39)$$

$$R_{\tau_{ij}}^k = \tau_{ij}^k - \tau_{ij}^{k-1} \quad (40)$$

then residues are arithmetic mean of the whole $R_{\tau_{ij}}^k$ matrix

$$residue_{ij}^k = \text{mean}(R_{\tau_{ij}}^k) \quad (41)$$

Same principle had been applied to pressure residue.

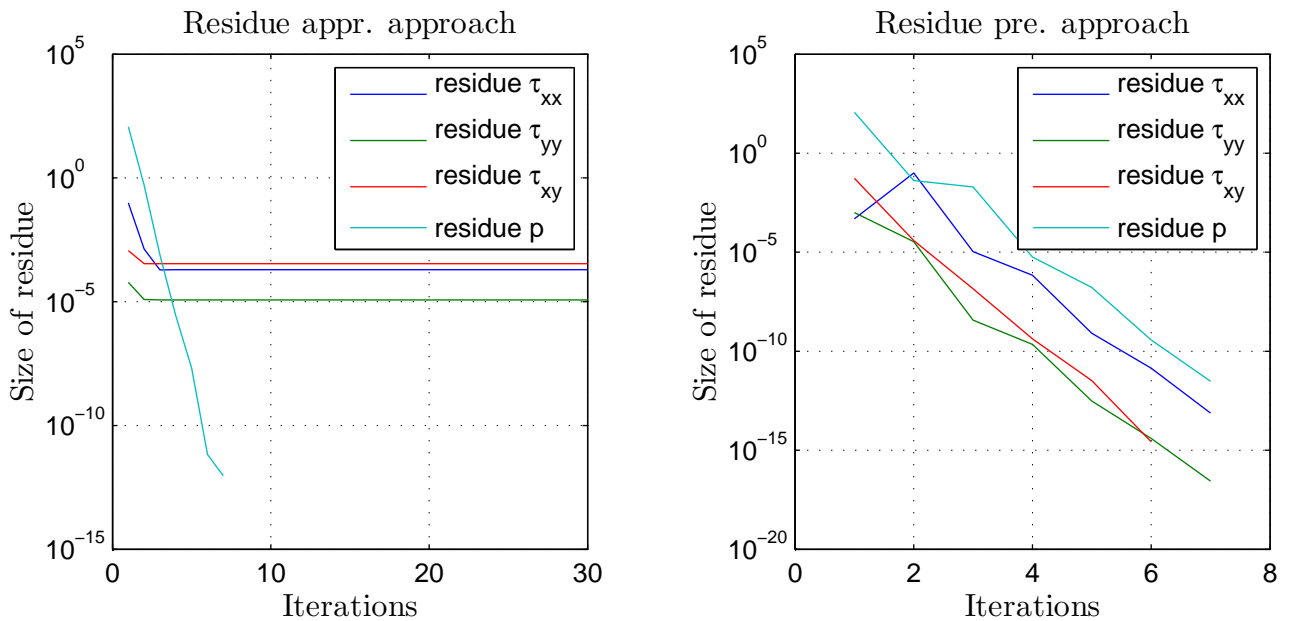


Figure 6 Residue for "approximation" approach and "predictor" approach.

Pressure

The main goal was to find the pressure in convergent divergent planar channel. Pressure can be compared in the future with experimental data. There exist significant peak of pressure in the middle of planar channel, parallel to ξ -axis. It may be cost by the viscosity model or velocity field carried out by power model.

There is a difference between pressure field obtained by "approximation" and "predictor" approach, (see figure 7). This difference occurs on the top wall in the divergent segment and is around 700 Pa, which is less than 0.1%. As one can see in figure 6, approach using on border first approximation is not converging, so produced stress field is different and therefore must be pressure also different.

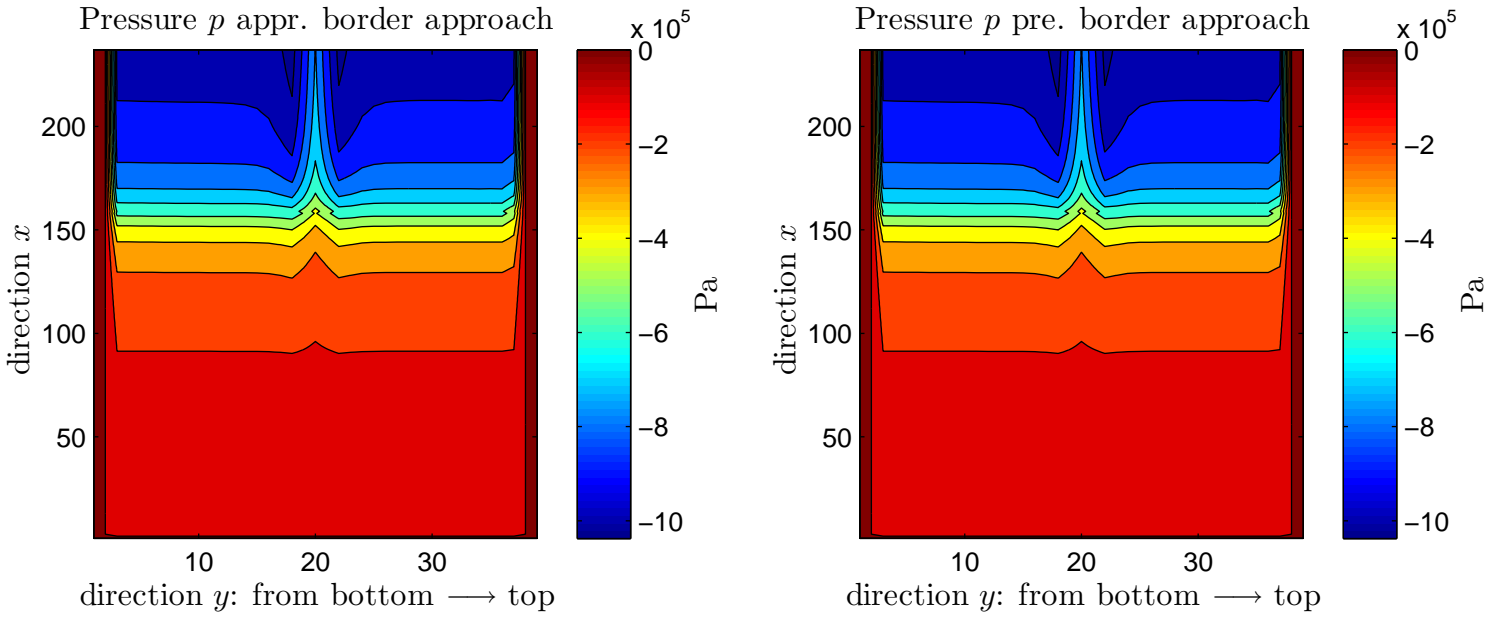


Figure 7 Pressure for "approximation" and "predictor" approach.

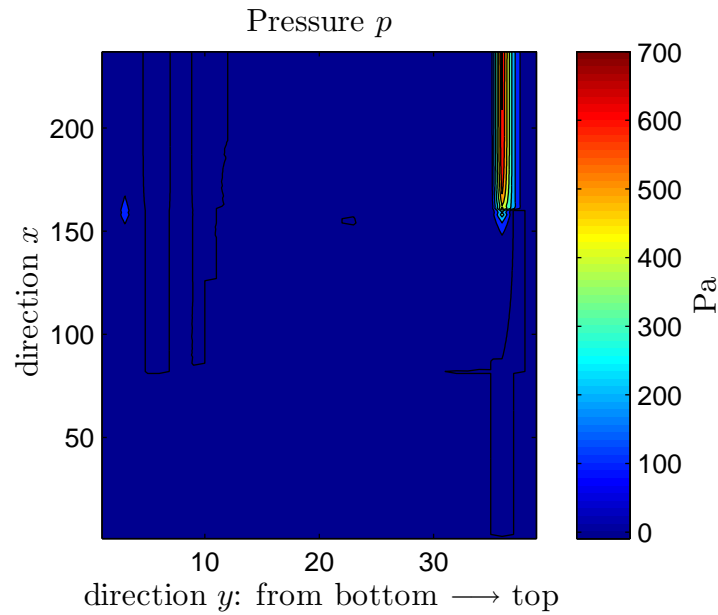


Figure 8 Pressure difference between "approximation" and "predictor" approach.

5 Conclusion

Results show significant peak of pressure in the middle of the channel. I have no explanation for this kind of behavior.

Although one would suspect second-order differences to converge faster, the opposite is true, they will quickly begin oscillating around 10^{-5} residues. This produces different stresses which cause difference between pressure calculated by first and second order differences.

It would be interesting to compare results obtained in this work with results obtained by some other CFD software. There are two widely used, well documented software solutions, which can be used for visco-elastic flow, OpenFoam and PolyFlow. OpenFoam is open-source, white-box software and it was selected to be applied for described problem

simulation. Parametric mesh for OpenFoam had been created manually in `BlockMeshDict` and transformed to mesh using `BlockMesh`. This work is ready for comparison with laboratory experiment.

Acknowledgements

This research was supported by research project GA CR No. 14-23482S (Thermal, electrical and rheological properties of collagen matter).

List of used symbols

L	length of segment	(m)
L_I	length of 1.st segment	(m)
H	height of segment	(m)
H_0	initial height	(m)
ΔH	difference of height	(m)
ΔL	current length of segment	(m)
ξ	dimensionless length (ξ -axis)	(1)
η	dimensionless height (η -axis)	(1)
ε	ratio between initial height and length of segment	(1)
β	contraction ratio	(1)
K	flow consistency index	(Pa·s ^{n})
n	flow behavior index	(1)
u_m	mean velocity	(m/s)
u	velocity	(m/s)
p	pressure	(Pa)
τ_{ij}	ij component of stress tensor	(Pa)
G	Shear modulus	(Pa)
μ	dynamic viscosity	(Pa·s)
u_i	velocity in i direction	(m/s)

References

- [1] RD Harkness. Biological functions of collagen. *Biological reviews of the Cambridge Philosophical society*, 36(4):399-&, 1961.
- [2] CH Lee, A Singla and Y Lee. Biomedical applications of collagen. *International journal of pharmaceutics*, 221(1-2):1-22, 2001.
- [3] K Gelse, E Poschl and T Aigner. Collagens - structure, function, and biosynthesis. *Advanced drug delivery reviews*, 55(12):1531-1546, 2003.
- [4] R. Žitný, M. Houska, A. Landfeld, J. Skocilas and J. Stancl. Possible explanations of hysteresis at hydraulic characteristics in pipes. In *CHISA 2014*, pages 14, Praha, 2014.
- [5] R. Žitný. Metzner-white convergent divergent planar channel flow. 2014.
- [6] S. Solnář. Figure of the convergent divergent planar channel viscosimetr [figure], (archive of the author). 2015
- [7] J. Pavlovec. Výtlačný reometr pro viskoelastické kapaliny. Praha, 1991
- [8] P. Getreuer. Writing fast matlab code. 2004